Open access • Journal Article • DOI:10.1007/S11340-006-9659-3

Mechanical Properties of Microcapsules Used in a Self-Healing Polymer

Michael W. Keller, Nancy R. Sottos

Institutions: University of Illinois at Urbana–Champaign

Published on: 23 Nov 2006 - Experimental Mechanics (Kluwer Academic Publishers)

Topics: Elastic modulus

Mechanical Properties of Microcapsules Used in a Self-Healing Polymer

M.W. Keller* and N.R. Sottos†

Department of Theoretical and Applied Mechanics

and

Beckman Institute for Advanced Science and Technology

University of Illinois at Urbana-Champaign,

Urbana, IL 61801

(Dated: September 6, 2005)

Abstract

The elastic modulus and failure behavior of poly(urea-formaldehyde) shelled microcapsules were determined through single-capsule compression tests. Capsules were tested both dry and immersed in a fluid isotonic with the encapsulant. A shell-theory model for a fluid-filled microcapsule was utilized to extract the modulus of the shell wall material from individual capsule tests. The testing of capsules immersed in a fluid had little influence on mechanical behavior in the elastic regime. The average capsule shell wall modulus was determined to be 3.7 GPa. Capsule diameter was found to have a significant effect on burst strength, with smaller capsules sustaining higher stresses before burst.

*mwkeller@uiuc.edu

†n-sottos@uiuc.edu

I. INTRODUCTION

Microcapsules containing liquid healing agent are a critical component of self-healing polymers [1, 2]. Healing is accomplished by incorporating the microencapsulated healing agent and a catalyst within an epoxy matrix. An approaching crack ruptures embedded microcapsules, releasing healing agent into the crack plane through capillary action. Polymerization of the healing agent is initiated by contact with the embedded chemical catalyst, bonding the crack faces. The rupture of microcapsules is the mechanical trigger to the healing process and without it, no healing occurs. This system has proven to be highly effective at healing cracks in both quasi-static [1] and fatigue [3–6] loading.

An optimal combination of microcapsule and matrix properties is necessary to ensure mechanical triggering when the material is damaged; if the shell wall is too thick the microcapsule will not rupture readily, preventing the release of healing agent. On the other hand, if the shell wall is too thin, the capsules not only are fragile, but also allow diffusion of the healing agent into the matrix. Other key parameters for efficient healing agent delivery are the elastic stiffness, the fill content, and the burst strength of the capsules.

The complex three-dimensional crack–microcapsule interaction which occurs in a self-healing composite has been studied using the Eshelby–Mura equivalent inclusion method [1]. Model predictions reveal that that the capsule-to-matrix stiffness ratio influences the crack propagation path in close proximity to the capsule. A capsule with a higher elastic modulus than the surrounding matrix creates a stress field that tends to deflect the crack away from the microcapsule. Conversely, a more compliant shell wall material produces a stress field that attracts the crack toward the microcapsule, facilitating capsule rupture.

In addition to providing storage of the healing monomer, Brown et al. [7] demonstrated that microcapsules toughen the polymer matrix by as much as 127% over the neat matrix (with no capsules) value. Previous studies of microcapsule toughening included only the effect of average capsule diameter and volume faction. The additional influences of shell wall thickness, capsule processing, and fill content on toughening in a polymer matrix were examined in more recent work [8]. While all three of these parameters significantly impacted the efficiency of microcapsule toughening, it was difficult to elucidate the relationship between physical properties of the microcapsule and the fracture performance of the polymer composite. The goal of the present work is to characterize the mechanical properties of the microcapsule system currently used in self-healing composites.

Several methods for characterizing capsules have appeared in the literature, most of which were developed for biological cells. Mitchison and Swan [9] introduced a micropipette aspiration test for probing the mechanical response biological cells. A micropipette was placed in contact with the cell and a vacuum was applied, drawing the cell wall into the micropipette. The cell wall deflection was measured and related to the mechanical stiffness of the wall material. The micropipette aspiration technique has also been applied to determine microcapsule shell wall elastic modulus [10]. Cole used a simple compression test to characterize the stiffness of sea urchin eggs [11]. A single egg was placed between two platens and then compressed. In addition to characterizing biological cells, this experimental technique has been applied to microcapsule systems [12–14]. In the current work, the single-capsule compression experiment is adopted for the characterization of a range of microcapsules and the resulting load–displacement data compared with a shell theory model to determine the elastic properties of the shell wall.

II. EXPERIMENTAL PROCEDURE

A. Capsule Manufacture

The capsules examined in this study had a poly(urea-formaldehyde)(UF) shell wall and were filled with dicyclopentadiene (DCPD) liquid monomer. They were identical to those used for the self-healing system in [1] and were manufactured by an *in-situ* microencapsulation method. *In-situ* microencapsulation proceeds in two concurrent steps. First a UF prepolymer is formed in an aqueous bath containing an emulsified, water-immiscible encapsulent fluid [15]. The UF polymerizes around an individual DCPD droplet in the emulsion, forming the shell wall of an individual microcapsule. Capsule diameter is determined by the droplet size of the emulsion. A schematic of the manufacture procedure for UF capsules is presented in Fig. 1. The average diameters for each capsule group tested were 213±12 μm, 187±15 μm, and 65±7 μm.

A representative scanning electron microscopy (SEM) micrograph of the surface morphology of a UF capsule is shown in Fig. 2. In addition to allowing investigation of surface morphology, SEM allowed measurement of the shell wall thickness of an individual capsule. These microcapsules possessed a highly uniform shell wall thickness, 175±33 nm, independent of capsule diameter.

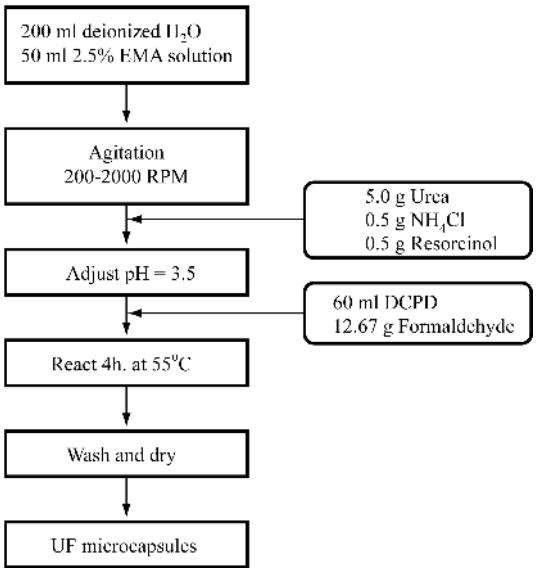

FIG. 1: Encapsulation procedure for UF capsules [15]

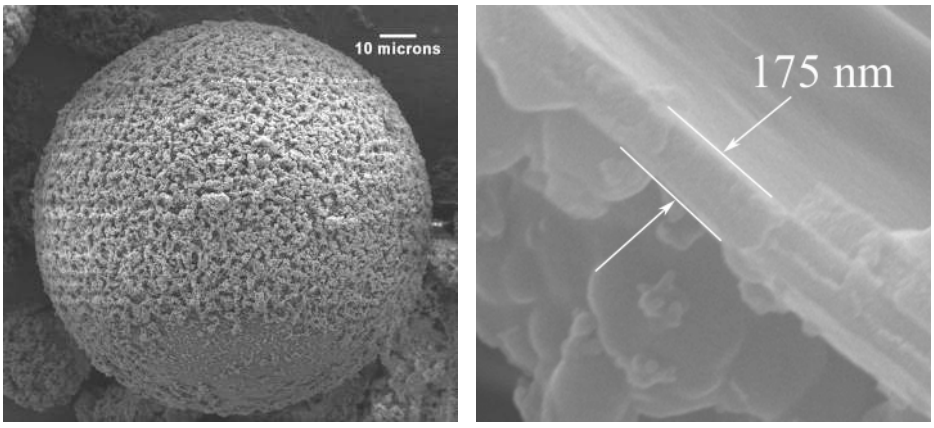

(a) (b)

FIG. 2: Electron micrographs of a UF DCPD filled microcapsule: (a) surface morphology; (b) cross-section of the shell wall.

B. Experimental Setup

The capsule compression apparatus, shown in Fig. 3, was adapted from the one described by Liu and coworkers [12]. Displacement was applied at a rate of 5 μm/s for the 187 μm and 213 μm capsule size ranges and 2.5 μm/s for the 65 μm size range using a stepper actuator (Physik Insturmente M-230S) controlled via a computer interface. Load data were acquired from a 10 g load cell (Transducer Techniques GSO-10) via a DAQ card (PCI-MIO-16E-4) and associated software from National Instruments. Images of the capsule during the compression cycle were captured through a stereo microscope (Nikon SMZ-2T)

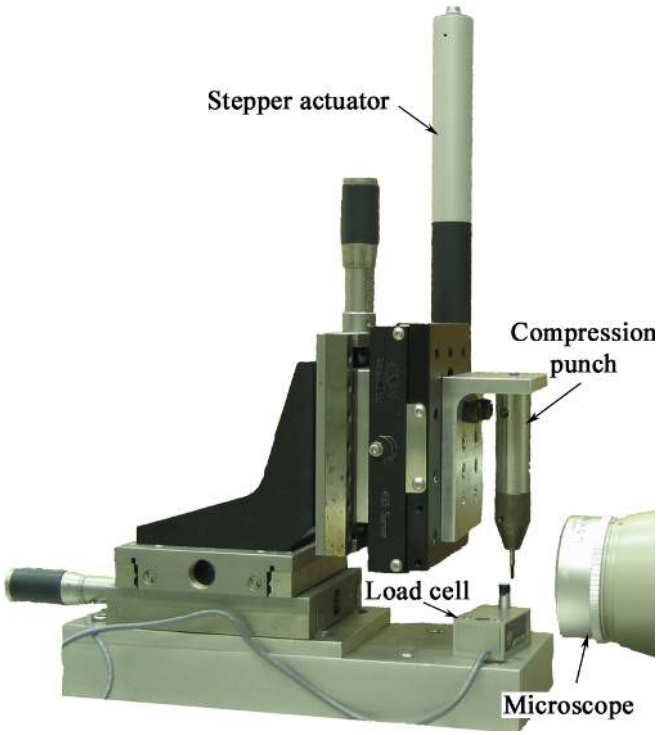

FIG. 3: Photograph of experimental setup.

by a monochrome CCD Camera (Qimaging Retiga). The entire system was mounted on a vibration isolation table.

For a dry microcapsule test, capsules were drawn into a pipette, which enabled release of a single capsule onto the compression platen. An image of the microcapsule was taken prior to compression to determine the initial capsule diameter. An initial separation between the capsule and punch allowed the stepper to achieve steady-state velocity after motion was initiated. The test program was started after positioning the punch above the capsule and terminated after burst was observed.

Immersion tests were conducted using a modification of the apparatus presented in Fig. 3. A schematic of the modified compression setup and the immersion test cell are shown in Fig. 4. Capsules tested in the immersion setup were dispersed in a bath of DCPD and allowed to equilibrate for at least 24 hours. Then a single capsule was removed from solution by pipetting and placed into the compression cell. Fluid was added to the cell cavity to ensure that the entire capsule was submerged. Testing then proceeded as described for the dry test.

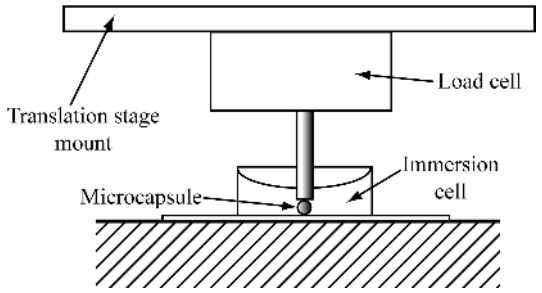

FIG. 4: Schematic of the immersion testing apparatus.

III. COMPRESSION TEST RESULTS

Figure 5 shows representative load–displacement data for an immersed capsule, 213 μm in diameter, tested in compression. Dimensionless displacement is defined by the displacement, δ, divided by the initial capsule diameter, D. Capsules tested while immersed in the encapsulant fluid were imaged by backlighting. In Fig. 5 the images numbered one through four show the capsule during representative sections of the loading sequence. In these images, the solid white line indicates the bottom of the compression platen and the dark region is the compression punch. Image 1 shows the capsule prior to contact with the compression platen. Image 2 is the capsule near the 15% dimensionless displacement point. At approximately this displacement, other researchers have observed a 'yield' in the load–displacement response. This yield is characterized by a change in concavity of the load–displacement curve [13]. Image 3 captures the capsule near the 'burst' event, which is indicated by the load peak, and image 4 is the capsule after burst.

From Fig. 5 two key observations of compressive capsule shell wall behavior are evident: the capsule shell wall does not buckle during compression and, the capsule remains effectively intact after burst. The absence of buckling indicates that the yield point is due to localized damage, such as microcracking or shear yielding, of the shell wall material. The burst event was also studied with dry compression tests utilizing capsules filled with dyed DCPD. Capsule burst was observed to proceed from the edge of the contact zone where the radius of curvature is the highest. This burst is not a dynamic event, but a leaking of encapsulant fluid from a shell wall failure. The encapsulent leakage proceeds quickly, coating the surface of the capsule in a few seconds.

Figure 6 is a comparison of compression results for dry and immersed capsules of similar diameters. The load–displacement responses of these tests are quite similar in the elastic

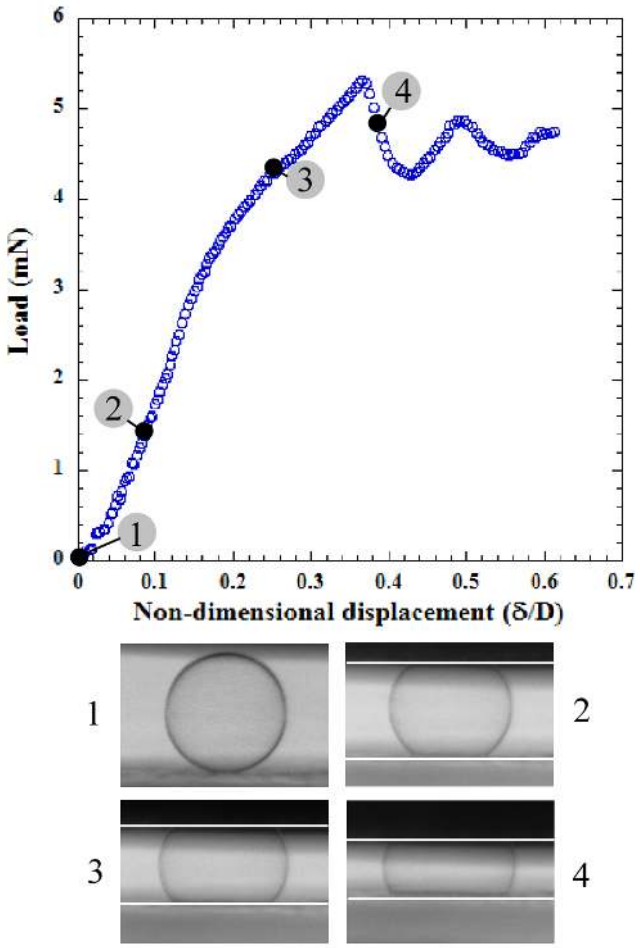

FIG. 5: Images of a 213 μm diameter capsule during an immersed compression test.

region of the test (dimensionless displacement less than 15%). At about 20% dimensionless displacement, however, the capsule response changes. The dry capsules generally sustain more load prior to burst than the immersed capsules.

Capsules from batches with average diameters of 187±15 μm and 65±7 μm were tested in dry compression to determine the effect of capsule size. Figure 7 shows representative load–displacement responses for each of the capsule diameters. Two size effects can be noted: smaller capsules are less stiff as a system, in the sense that they sustain less load for a given dimensionless displacement, and the maximum load at burst is highly diameter dependent. The dependence of burst strength on capsule diameter has been observed previously [13]. Table I shows the average burst force and burst strength of the microcapsule types tested. The burst strength is calculated as the burst force normalized by capsule cross-sectional area. The strength data indicate that during dry compression, smaller capsules are harder

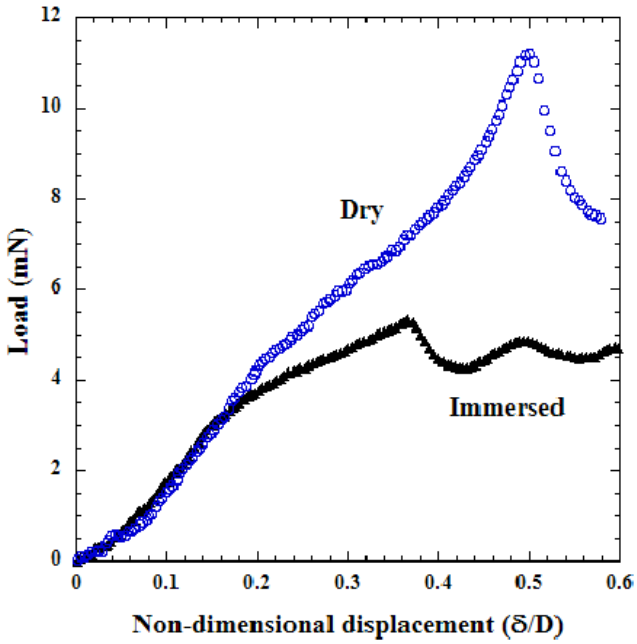

FIG. 6: Comparison of dry and immersed tests on capsules of similar diameter (222 μm).

to burst than their larger counterparts.

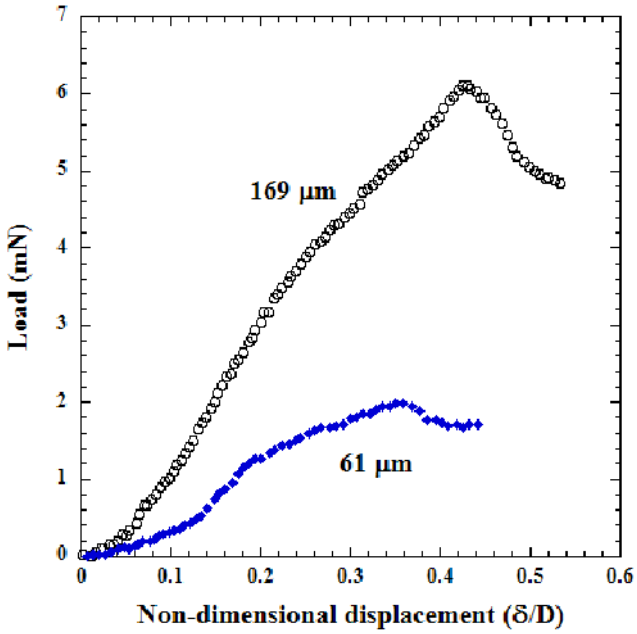

FIG. 7: Comparison of load–displacement responses for a 169 μm diameter microcapsule and a 61 μm diameter microcapsule tested in dry compression.

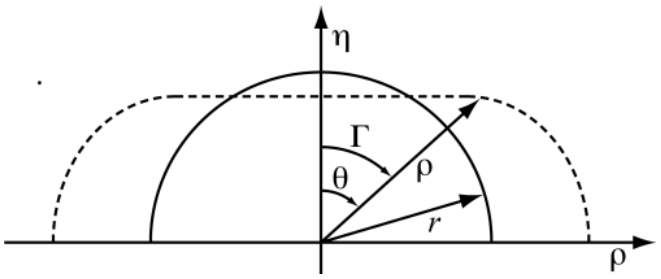

FIG. 8: Schematic of the microcapsule compression problem. The solid line is the uncompressed microcapsule and the dashed line is the compressed microcapsule, after the figure in [12].

IV. COMPARISON WITH THEORY

A. Model Development

The elastic modulus of the capsule shell wall material is extracted through comparison with an analytical membrane theory model. The model is based on the theory initially developed by Feng and Yang [16] for an inflated spherical membrane and then later extended to fluid-filled shells by Lardner and Pujara [17]. The current work follows the analysis for fluid-filled shells as presented in [18] that includes a linear elastic constitutive relationship for the shell wall material. A summary of the model is presented below along with comparisons with the current compression data.

The compression of a microcapsule is shown schematically in Fig. 8, where the solid line is the uncompressed profile and the dashed line represents the compressed geometry. This geometrical arrangement generates two systems of ODEs, one for each distinct region of the compressed capsule. The contact region, the flat portion of the dashed profile, is constrained in one dimension by the compression punch. The non-contact region, which comprises the rest of the capsule shell, is unconstrained and can deform freely.

The system of ODEs for the contact region are

$$\lambda_1^{'} = -\frac{\lambda_1}{\lambda_2 \sin\psi}\frac{f_3}{f_1} - \frac{\lambda_1 - \lambda_2\cos\psi}{\sin\psi}\frac{f_2}{f_1}, \tag{1}$$

$$\lambda_2^{'} = \frac{\lambda_1 - \lambda_2\cos\psi}{\sin\psi}, \tag{2}$$

where ψ is the angular coordinate of the compressed capsule, λ_1 and λ_2 are the principal

stretch ratios, and f_1, f_2, and f_3 are

$$f_1 = \frac{\partial T_1}{\partial \lambda_1}, \tag{3}$$

$$f_2 = \frac{\partial T_2}{\partial \lambda_2}, \tag{4}$$

$$f_3 = T_1 - T_2, \tag{5}$$

where T_1 and T_2 are the membrane tensions.

The ODEs for the non-contact region are

$$\lambda_1^{'} = \frac{\delta \cos\psi - \omega \sin\psi}{\sin^2\psi}\frac{f_2}{f_1} - \frac{\omega}{\delta}\frac{f_3}{f_1}, \tag{6}$$

$$\delta^{'} = \omega \tag{7}$$

$$\omega^{'} = \frac{\lambda_1^{'}\omega}{\lambda_1} + \frac{\lambda_1^2 - \omega^2}{\delta}\frac{T_2}{T_1} - \frac{\lambda_1(\lambda_1^2 - \omega^2)^{1/2} Pr_0}{T_1}, \tag{8}$$

where

$$\delta = \lambda_2 \sin\psi. \tag{9}$$

A linear elastic constitutive relationship was assumed for the current microcapsule systems and was derived following [18]. The linear-elastic strain energy formula is

$$W = \frac{Eh_0}{2\left(1+\nu^2\right)}\Big\{(\lambda_1 - 1)^2 + (\lambda_2 - 1)^2 + 2\nu(\lambda_1 - 1)(\lambda_2 - 1)\Big\} \tag{10}$$

from [19]. The wall tensions T_i are related to the strain energy by

$$T_i = \frac{1}{\lambda_1\lambda_2}\frac{\partial W}{\partial \lambda_i}(\lambda_i)^2. \tag{11}$$

Equation (10) with Eqn. (11) yields

$$T_1 = \frac{Eh_0}{(1-\nu^2)}\frac{\lambda_1}{\lambda_2}\left\{(\lambda_1 - 1) + \nu(\lambda_2 - 1)\right\}, \tag{12}$$

$$T_2 = \frac{Eh_0}{(1-\nu^2)}\frac{\lambda_2}{\lambda_1}\left\{(\lambda_2 - 1) + \nu(\lambda_1 - 1)\right\} \tag{13}$$

for the shell wall tensions. The boundary conditions for this problem are

$$\begin{aligned}
&\psi = 0: \quad \lambda_1 = \lambda_2 = \lambda_0, \\
&\psi = \Gamma: \quad \lambda_{1,\text{contact}} = \lambda_{1,\text{non}-\text{contact}}, \\
&\psi = \Gamma: \quad \lambda_{2,\text{contact}} = \lambda_{2,\text{non}-\text{contact}}, \\
&\psi = \Gamma: \quad \eta^{'} = 0, \\
&\psi = \frac{\pi}{2}: \quad \delta^{'} = 0.
\end{aligned} \tag{14}$$

The above system of ODEs were solved using the numerical scheme outlined in [16]. Numerical solutions were performed with a Runge–Kutta solver provided by Matlab (The MathWorks Inc.). Input to this program consisted of the measured capsule diameter and the average wall thickness. The Poisson's ratio ν was assumed to be 1/3, a value consistent with other formaldehyde-based polymers. Since the problem is time independent, the load–displacement plots were generated by solving the equilibrium problem of the capsule for a given contact radius and determining the corresponding cross-head displacement.

A sensitivity study was undertaken to investigate the influence of Poisson's ratio variance on the calculated load–displacement response. Figure 9(a) shows the non-dimensional force ($F = P/Eh_0r_0$)–dimensionless displacement response for different values of the Poisson's ratio. The model exhibits little sensitivity to Poisson's ratio, and the results shown in Fig. 9(a) are independent of capsule diameter or shell wall thickness. The sensitivity to shell wall thickness variation was also investigated numerically. Figure 9(b) contains predicted load–displacement curves for a hypothetical capsule with a diameter of 180 μm and a shell wall modulus of 3.6 GPa. The family of curves are the calculated load–displacement responses if the shell wall is assumed to be the average thickness, the upper thickness limit, and the lower thickness limit measured by SEM on a microcapsule batch. These numerical studies indicate that variation in the shell wall thickness alters the predicted modulus value by the same percentage as the thickness variation. That is, if the shell wall is assumed to be 20% thicker than the actual value, the modulus will be under-predicted by 20%. Additionally, the encapsulated volume is assumed constant, as in previous studies [12, 17]. The constant volume assumption disallows fluid diffusion through the shell wall.

B. Property Extraction

Representative model fits for a 169 μm capsule and a 61 μm capsule tested in dry compression are shown in Fig. 10(a). The model was fit to the experimental data using Young's modulus as the single adjustable parameter. Modulus values obtained from both dry and immersed compression tests are summarized in Table I. The model fits show good agreement until the capsules reach displacement values near 15% (yield point) and then the model deviates significantly from the experimental data. The model predicts a maximum of 3 to 4 percent strain in the capsule shell wall at this point. Strains of this magnitude are sufficient to initiate damage in other thermosetting polymers and, as mentioned previously, the

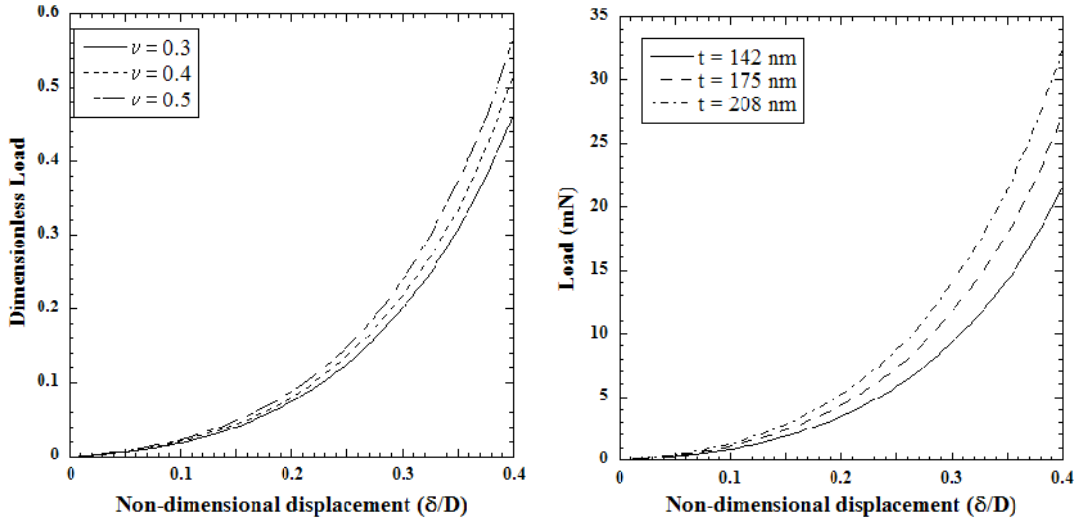

(a) (b)

FIG. 9: load–displacement plots from model parameter studies on the (a) effect of Poisson's ratio ($t = 175$ nm) (b) effect of shell wall thickness variation for a hypothetical 180 μm capsule with a shell wall modulus of 3.6 GPa.

TABLE I: Average Young's modulus and burst behavior of tested microcapsules.

Average diameter (μm $\pm$Std. dev.)	t/D	E (GPa $\pm$Std. dev.)	Average burst force (mN $\pm$Std. dev.)	Normalized burst strength (MPa $\pm$Std. dev.)
187$\pm$15, dry	0.001	3.6 ± 0.4	6.5 ± 1.6	0.24 ± 0.04
213$\pm$12, immersed	0.001	3.9 ± 0.7	4.9 ± 0.5	0.14 ± 0.02
65$\pm$7, dry	0.004	3.7 ± 0.5	2.7 ± 0.7	0.8 ± 0.3

yield point may indicate the onset of damage in the shell wall. Dye tests have indicated that there is significant leakage of encapsulant fluid only near 45% deformation, but some diffusion of encapsulant fluid may be occurring. This diffusion would have an effect on the load–displacement behavior of the capsules and is not accounted for in the model. A representative model fit for the compression of a 223 μm immersed capsule, Fig. 10(b), shows similar behavior to the dry tests. In this case, the model again deviates just prior to 15% deformation.

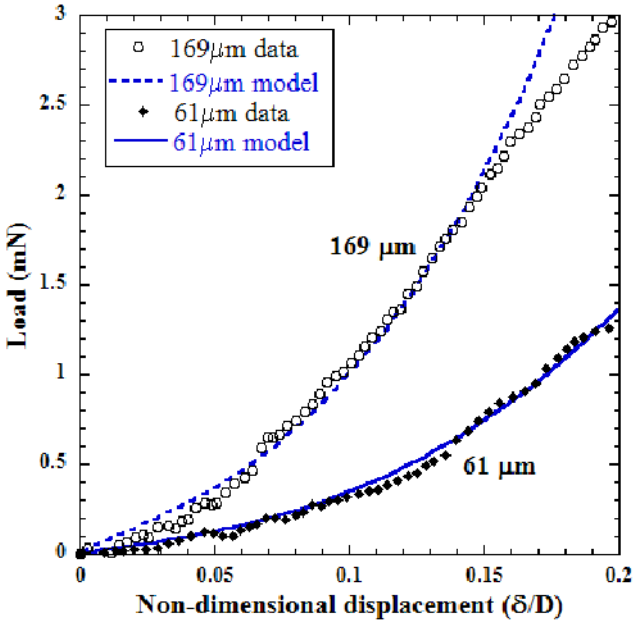

(a) Model comparisons for dry compression tests.

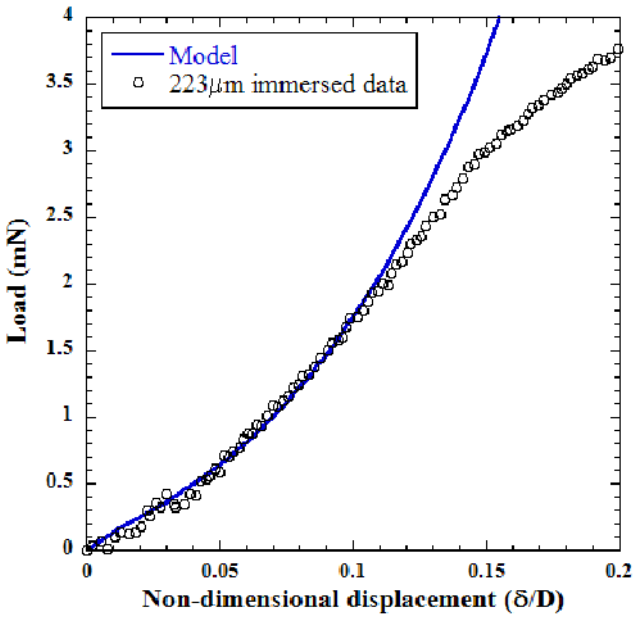

(b) Model comparison for an immersed test.

FIG. 10: Comparisons of experimental load–displacement data with the fluid-filled model for dry and immersed UF capsules.

V. CONCLUSIONS

The shell wall elastic modulus of poly(urea-formaldehyde) shelled microcapsules was successfully extracted from single capsule compression testing by comparison with a membrane theory model. Young's modulus was found to have an average value of 3.7±0.2 GPa for all

capsule testing conditions and was independent of capsule diameter. However, capsule burst behavior was found to be highly diameter dependent. Capsules of smaller diameters, while bursting at lower loads, have a higher specific strength.

Acknowledgments

The authors would like to acknowledge support from the National Science Foundation (Grant NSF CMS 02-18863) and NASA/JPL (subcontract 1270900). The electron microscopy was performed with the assistance of S. Robinson in the Imaging Technology Group at the Beckman Institute, University of Illinois Urbana-Champaign. The authors would also like to thank Prof. S.R. White and Prof. G. Gioia for fruitful discussions.

---

[1] S. White, N. Sottos, P. Geubelle, J. Moore, M. Kessler, S. Sriram, E. Brown, and S. Viswanathan, Nat. **409**, 794 (2001).

[2] E. Brown, S. White, and N. Sottos, Exp. Mech. **42**, 372 (2002).

[3] E. Brown, Ph.D. thesis, Department of Theoretical and Applied Mechanics, University of Illinois Urbana-Champaign (2003).

[4] E. Brown, S. White, and N. Sottos, Compos. Sci. Technol. (2005), to appear.

[5] E. Brown, S. White, and N. Sottos, Compos. Sci. Technol. (2005), to appear.

[6] E. Brown, S. White, and N. Sottos, J. Mat. Sci. (2005), in review.

[7] E. Brown, S. White, and N. Sottos, J. Mat. Sci. **39**, 1703 (2004).

[8] M. Keller and N. Sottos, in *Proceedings of the 2004 SEM X International Congress on Experimental and Applied Mechanics* (2004).

[9] J. Mitchison and M. Swan, J. Exp. Biol. **32**, 443 (1954).

[10] A. Jay and M. Edwards, Can. J. Physiol. Pharmacol. **46**, 731 (1968).

[11] K. Cole, J. Cell Comp. Physiol. **1**, 1 (1937).

[12] K. Liu, D. Williams, and B. Briscoe, Phys. Rev. E **54**, 6673 (1996).

[13] G. Sun and Z. Zhang, Int. J. Pharm. **242**, 303 (2004).

[14] Z. Zhang, R. Saunders, and C. Thomas, J. Microencap. **16**, 117 (1999).

[15] E. Brown, M. Kessler, N. Sottos, and S. White, J. Microencap. **20**, 719 (2003).

[16] W. Feng and W. Yang, J. Appl. Mech. **40**, 209 (1973).

[17] T. Lardner and P. Pujara, in *Mechanics Today*, edited by S. Nemat-Nassar (Pergamon, 1980), pp. 161–176.

[18] C. Wang, L. Wang, and C. Thomas, Ann. Botany **93**, 443 (2004).

[19] L. Cheng, J. Biomed. Eng. **109**, 10 (1987).

List of Recent TAM Reports

No.	Authors	Title	Date
989	Riahi, D. N.	On stationary and oscillatory modes of flow instabilities in a rotating porous layer during alloy solidification—*Journal of Porous Media* **6**, 1–11 (2003)	Nov. 2001
990	Okhuysen, B. S., and D. N. Riahi	Effect of Coriolis force on instabilities of liquid and mushy regions during alloy solidification—*Physics of Fluids* (submitted)	Dec. 2001
991	Christensen, K. T., and R. J. Adrian	Measurement of instantaneous Eulerian acceleration fields by particle-image accelerometry: Method and accuracy—*Experimental Fluids* (submitted)	Dec. 2001
992	Liu, M., and K. J. Hsia	Interfacial cracks between piezoelectric and elastic materials under in-plane electric loading—*Journal of the Mechanics and Physics of Solids* **51**, 921–944 (2003)	Dec. 2001
993	Panat, R. P., S. Zhang, and K. J. Hsia	Bond coat surface rumpling in thermal barrier coatings—*Acta Materialia* **51**, 239–249 (2003)	Jan. 2002
994	Aref, H.	A transformation of the point vortex equations—*Physics of Fluids* **14**, 2395–2401 (2002)	Jan. 2002
995	Saif, M. T. A, S. Zhang, A. Haque, and K. J. Hsia	Effect of native Al_2O_3 on the elastic response of nanoscale aluminum films—*Acta Materialia* **50**, 2779–2786 (2002)	Jan. 2002
996	Fried, E., and M. E. Gurtin	A nonequilibrium theory of epitaxial growth that accounts for surface stress and surface diffusion—*Journal of the Mechanics and Physics of Solids* **51**, 487–517 (2003)	Jan. 2002
997	Aref, H.	The development of chaotic advection—*Physics of Fluids* **14**, 1315–1325 (2002); see also *Virtual Journal of Nanoscale Science and Technology*, 11 March 2002	Jan. 2002
998	Christensen, K. T., and R. J. Adrian	The velocity and acceleration signatures of small-scale vortices in turbulent channel flow—*Journal of Turbulence*, in press (2002)	Jan. 2002
999	Riahi, D. N.	Flow instabilities in a horizontal dendrite layer rotating about an inclined axis—*Journal of Porous Media*, in press (2003)	Feb. 2002
1000	Kessler, M. R., and S. R. White	Cure kinetics of ring-opening metathesis polymerization of dicyclopentadiene—*Journal of Polymer Science A* **40**, 2373–2383 (2002)	Feb. 2002
1001	Dolbow, J. E., E. Fried, and A. Q. Shen	Point defects in nematic gels: The case for hedgehogs—*Archive for Rational Mechanics and Analysis* **177**, 21–51 (2005)	Feb. 2002
1002	Riahi, D. N.	Nonlinear steady convection in rotating mushy layers—*Journal of Fluid Mechanics* **485**, 279–306 (2003)	Mar. 2002
1003	Carlson, D. E., E. Fried, and S. Sellers	The totality of soft-states in a neo-classical nematic elastomer—*Journal of Elasticity* **69**, 169–180 (2003) with revised title	Mar. 2002
1004	Fried, E., and R. E. Todres	Normal-stress differences and the detection of disclinations in nematic elastomers—*Journal of Polymer Science B: Polymer Physics* **40**, 2098–2106 (2002)	June 2002
1005	Fried, E., and B. C. Roy	Gravity-induced segregation of cohesionless granular mixtures—*Lecture Notes in Mechanics*, in press (2002)	July 2002
1006	Tomkins, C. D., and R. J. Adrian	Spanwise structure and scale growth in turbulent boundary layers—*Journal of Fluid Mechanics* (submitted)	Aug. 2002
1007	Riahi, D. N.	On nonlinear convection in mushy layers: Part 2. Mixed oscillatory and stationary modes of convection—*Journal of Fluid Mechanics* **517**, 71–102 (2004)	Sept. 2002
1008	Aref, H., P. K. Newton, M. A. Stremler, T. Tokieda, and D. L. Vainchtein	Vortex crystals—*Advances in Applied Mathematics* **39**, in press (2002)	Oct. 2002
1009	Bagchi, P., and S. Balachandar	Effect of turbulence on the drag and lift of a particle—*Physics of Fluids*, in press (2003)	Oct. 2002
1010	Zhang, S., R. Panat, and K. J. Hsia	Influence of surface morphology on the adhesive strength of aluminum/epoxy interfaces—*Journal of Adhesion Science and Technology* **17**, 1685–1711 (2003)	Oct. 2002

List of Recent TAM Reports (cont'd)

No.	*Authors*	*Title*	*Date*
1011	Carlson, D. E., E. Fried, and D. A. Tortorelli	On internal constraints in continuum mechanics—*Journal of Elasticity* **70**, 101–109 (2003)	Oct. 2002
1012	Boyland, P. L., M. A. Stremler, and H. Aref	Topological fluid mechanics of point vortex motions—*Physica D* **175**, 69–95 (2002)	Oct. 2002
1013	Bhattacharjee, P., and D. N. Riahi	Computational studies of the effect of rotation on convection during protein crystallization—*International Journal of Mathematical Sciences*, in press (2004)	Feb. 2003
1014	Brown, E. N., M. R. Kessler, N. R. Sottos, and S. R. White	*In situ* poly(urea-formaldehyde) microencapsulation of dicyclopentadiene—*Journal of Microencapsulation* (submitted)	Feb. 2003
1015	Brown, E. N., S. R. White, and N. R. Sottos	Microcapsule induced toughening in a self-healing polymer composite—*Journal of Materials Science* (submitted)	Feb. 2003
1016	Kuznetsov, I. R., and D. S. Stewart	Burning rate of energetic materials with thermal expansion—*Combustion and Flame* (submitted)	Mar. 2003
1017	Dolbow, J., E. Fried, and H. Ji	Chemically induced swelling of hydrogels—*Journal of the Mechanics and Physics of Solids*, in press (2003)	Mar. 2003
1018	Costello, G. A.	Mechanics of wire rope—Mordica Lecture, Interwire 2003, Wire Association International, Atlanta, Georgia, May 12, 2003	Mar. 2003
1019	Wang, J., N. R. Sottos, and R. L. Weaver	Thin film adhesion measurement by laser induced stress waves—*Journal of the Mechanics and Physics of Solids* (submitted)	Apr. 2003
1020	Bhattacharjee, P., and D. N. Riahi	Effect of rotation on surface tension driven flow during protein crystallization—*Microgravity Science and Technology* **14**, 36–44 (2003)	Apr. 2003
1021	Fried, E.	The configurational and standard force balances are not always statements of a single law—*Proceedings of the Royal Society* (submitted)	Apr. 2003
1022	Panat, R. P., and K. J. Hsia	Experimental investigation of the bond coat rumpling instability under isothermal and cyclic thermal histories in thermal barrier systems—*Proceedings of the Royal Society of London A* **460**, 1957–1979 (2003)	May 2003
1023	Fried, E., and M. E. Gurtin	A unified treatment of evolving interfaces accounting for small deformations and atomic transport: grain-boundaries, phase transitions, epitaxy—*Advances in Applied Mechanics* **40**, 1–177 (2004)	May 2003
1024	Dong, F., D. N. Riahi, and A. T. Hsui	On similarity waves in compacting media—*Horizons in World Physics* **244**, 45–82 (2004)	May 2003
1025	Liu, M., and K. J. Hsia	Locking of electric field induced non-180° domain switching and phase transition in ferroelectric materials upon cyclic electric fatigue—*Applied Physics Letters* **83**, 3978–3980 (2003)	May 2003
1026	Liu, M., K. J. Hsia, and M. Sardela Jr.	In situ X-ray diffraction study of electric field induced domain switching and phase transition in PZT-5H—*Journal of the American Ceramics Society* (submitted)	May 2003
1027	Riahi, D. N.	On flow of binary alloys during crystal growth—*Recent Research Development in Crystal Growth*, in press (2003)	May 2003
1028	Riahi, D. N.	On fluid dynamics during crystallization—*Recent Research Development in Fluid Dynamics*, in press (2003)	July 2003
1029	Fried, E., V. Korchagin, and R. E. Todres	Biaxial disclinated states in nematic elastomers—*Journal of Chemical Physics* **119**, 13170–13179 (2003)	July 2003
1030	Sharp, K. V., and R. J. Adrian	Transition from laminar to turbulent flow in liquid filled microtubes—*Physics of Fluids* (submitted)	July 2003
1031	Yoon, H. S., D. F. Hill, S. Balachandar, R. J. Adrian, and M. Y. Ha	Reynolds number scaling of flow in a Rushton turbine stirred tank: Part I—Mean flow, circular jet and tip vortex scaling—*Chemical Engineering Science* (submitted)	Aug. 2003

List of Recent TAM Reports (cont'd)

No.	Authors	Title	Date
1032	Raju, R., S. Balachandar, D. F. Hill, and R. J. Adrian	Reynolds number scaling of flow in a Rushton turbine stirred tank: Part II—Eigen-decomposition of fluctuation—*Chemical Engineering Science* (submitted)	Aug. 2003
1033	Hill, K. M., G. Gioia, and V. V. Tota	Structure and kinematics in dense free-surface granular flow—*Physical Review Letters* **91**, 064302 (2003)	Aug. 2003
1034	Fried, E., and S. Sellers	Free-energy density functions for nematic elastomers—*Journal of the Mechanics and Physics of Solids* **52**, 1671–1689 (2004)	Sept. 2003
1035	Kasimov, A. R., and D. S. Stewart	On the dynamics of self-sustained one-dimensional detonations: A numerical study in the shock-attached frame—*Physics of Fluids* (submitted)	Nov. 2003
1036	Fried, E., and B. C. Roy	Disclinations in a homogeneously deformed nematic elastomer—*Nature Materials* (submitted)	Nov. 2003
1037	Fried, E., and M. E. Gurtin	The unifying nature of the configurational force balance—*Mechanics of Material Forces* (P. Steinmann and G. A. Maugin, eds.), in press (2003)	Dec. 2003
1038	Panat, R., K. J. Hsia, and J. W. Oldham	Rumpling instability in thermal barrier systems under isothermal conditions in vacuum—*Philosophical Magazine*, in press (2004)	Dec. 2003
1039	Cermelli, P., E. Fried, and M. E. Gurtin	Sharp-interface nematic–isotropic phase transitions without flow—*Archive for Rational Mechanics and Analysis* **174**, 151–178 (2004)	Dec. 2003
1040	Yoo, S., and D. S. Stewart	A hybrid level-set method in two and three dimensions for modeling detonation and combustion problems in complex geometries—*Combustion Theory and Modeling* (submitted)	Feb. 2004
1041	Dienberg, C. E., S. E. Ott-Monsivais, J. L. Ranchero, A. A. Rzeszutko, and C. L. Winter	Proceedings of the Fifth Annual Research Conference in Mechanics (April 2003), TAM Department, UIUC (E. N. Brown, ed.)	Feb. 2004
1042	Kasimov, A. R., and D. S. Stewart	Asymptotic theory of ignition and failure of self-sustained detonations—*Journal of Fluid Mechanics* (submitted)	Feb. 2004
1043	Kasimov, A. R., and D. S. Stewart	Theory of direct initiation of gaseous detonations and comparison with experiment—*Proceedings of the Combustion Institute* (submitted)	Mar. 2004
1044	Panat, R., K. J. Hsia, and D. G. Cahill	Evolution of surface waviness in thin films via volume and surface diffusion—*Journal of Applied Physics* (submitted)	Mar. 2004
1045	Riahi, D. N.	Steady and oscillatory flow in a mushy layer—*Current Topics in Crystal Growth Research*, in press (2004)	Mar. 2004
1046	Riahi, D. N.	Modeling flows in protein crystal growth—*Current Topics in Crystal Growth Research*, in press (2004)	Mar. 2004
1047	Bagchi, P., and S. Balachandar	Response of the wake of an isolated particle to isotropic turbulent cross-flow—*Journal of Fluid Mechanics* (submitted)	Mar. 2004
1048	Brown, E. N., S. R. White, and N. R. Sottos	Fatigue crack propagation in microcapsule toughened epoxy—*Journal of Materials Science* (submitted)	Apr. 2004
1049	Zeng, L., S. Balachandar, and P. Fischer	Wall-induced forces on a rigid sphere at finite Reynolds number—*Journal of Fluid Mechanics* (submitted)	May 2004
1050	Dolbow, J., E. Fried, and H. Ji	A numerical strategy for investigating the kinetic response of stimulus-responsive hydrogels—*Computer Methods in Applied Mechanics and Engineering* **194**, 4447–4480 (2005)	June 2004
1051	Riahi, D. N.	Effect of permeability on steady flow in a dendrite layer—*Journal of Porous Media*, in press (2004)	July 2004
1052	Cermelli, P., E. Fried, and M. E. Gurtin	Transport relations for surface integrals arising in the formulation of balance laws for evolving fluid interfaces—*Journal of Fluid Mechanics* (submitted)	Sept. 2004
1053	Stewart, D. S., and A. R. Kasimov	Theory of detonation with an embedded sonic locus—*SIAM Journal on Applied Mathematics* (submitted)	Oct. 2004

List of Recent TAM Reports (cont'd)

No.	*Authors*	*Title*	*Date*
1054	Stewart, D. S., K. C. Tang, S. Yoo, M. Q. Brewster, and I. R. Kuznetsov	Multi-scale modeling of solid rocket motors: Time integration methods from computational aerodynamics applied to stable quasi-steady motor burning—*Proceedings of the 43rd AIAA Aerospace Sciences Meeting and Exhibit* (January 2005), Paper AIAA-2005-0357 (2005)	Oct. 2004
1055	Ji, H., H. Mourad, E. Fried, and J. Dolbow	Kinetics of thermally induced swelling of hydrogels—*International Journal of Solids and Structures* (submitted)	Dec. 2004
1056	Fulton, J. M., S. Hussain, J. H. Lai, M. E. Ly, S. A. McGough, G. M. Miller, R. Oats, L. A. Shipton, P. K. Shreeman, D. S. Widrevitz, and E. A. Zimmermann	Final reports: Mechanics of complex materials, Summer 2004 (K. M. Hill and J. W. Phillips, eds.)	Dec. 2004
1057	Hill, K. M., G. Gioia, and D. R. Amaravadi	Radial segregation patterns in rotating granular mixtures: Waviness selection—*Physical Review Letters* **93**, 224301 (2004)	Dec. 2004
1058	Riahi, D. N.	Nonlinear oscillatory convection in rotating mushy layers—*Journal of Fluid Mechanics* (submitted)	Dec. 2004
1059	Okhuysen, B. S., and D. N. Riahi	On buoyant convection in binary solidification—*Journal of Fluid Mechanics* (submitted)	Jan. 2005
1060	Brown, E. N., S. R. White, and N. R. Sottos	Retardation and repair of fatigue cracks in a microcapsule toughened epoxy composite—Part I: Manual infiltration—*Composites Science and Technology* (submitted)	Jan. 2005
1061	Brown, E. N., S. R. White, and N. R. Sottos	Retardation and repair of fatigue cracks in a microcapsule toughened epoxy composite—Part II: *In situ* self-healing—*Composites Science and Technology* (submitted)	Jan. 2005
1062	Berfield, T. A., R. J. Ong, D. A. Payne, and N. R. Sottos	Residual stress effects on piezoelectric response of sol-gel derived PZT thin films—*Journal of Applied Physics* (submitted)	Apr. 2005
1063	Anderson, D. M., P. Cermelli, E. Fried, M. E. Gurtin, and G. B. McFadden	General dynamical sharp-interface conditions for phase transformations in viscous heat-conducting fluids—*Journal of Fluid Mechanics* (submitted)	Apr. 2005
1064	Fried, E., and M. E. Gurtin	Second-gradient fluids: A theory for incompressible flows at small length scales—*Journal of Fluid Mechanics* (submitted)	Apr. 2005
1065	Gioia, G., and F. A. Bombardelli	Localized turbulent flows on scouring granular beds—*Physical Review Letters*, in press (2005)	May 2005
1066	Fried, E., and S. Sellers	Orientational order and finite strain in nematic elastomers—*Journal of Chemical Physics* **123**, 044901 (2005)	May 2005
1067	Chen, Y.-C., and E. Fried	Uniaxial nematic elastomers: Constitutive framework and a simple application—*Proceedings of the Royal Society of London A* (submitted)	June 2005
1068	Fried, E., and S. Sellers	Incompatible strains associated with defects in nematic elastomers—*Physical Review Letters* (submitted)	Aug. 2005
1069	Gioia, G., and X. Dai	Surface stress and reversing size effect in the initial yielding of ultrathin films—*Journal of Applied Mechanics*, in press (2005)	Aug. 2005
1070	Gioia, G., and P. Chakraborty	Turbulent friction in rough pipes and the energy spectrum of the phenomenological theory—*arXiv:physics* 0507066 v1 8 Jul 2005	Aug. 2005
1071	Keller, M. W., and N. R. Sottos	Mechanical properties of capsules used in a self-healing polymer—*Experimental Mechanics* (submitted)	Sept. 2005